Heliyon 10 (2024) e37954

Contents lists available at ScienceDirect

Heliyon

journal homepage: www.cell.com/heliyon

Research article

The combined application of electromagnetic navigation and porcine fibrin sealant in microwave ablation of lung tumors

Jian Chen [a,b,1,*], Zaichun Shang [a,1], Pengfei Jia [c], Zhiming Chen [b], Xiaowen Cao [a], Xiao Han [d], Xinhua Zhang [a,***], Lou Zhong [a,d,**]

[a] Nantong University, Nantong, China
[b] Department of Radiation Oncology, Affiliated Hospital of Nantong University, Nantong, China
[c] Department of Interventional Radiology, Affiliated Hospital of Nantong University, Nantong, China
[d] Department of Thoracic Surgery, Affiliated Hospital of Nantong University, Nantong, China

ARTICLE INFO

Keywords:
Electromagnetic navigation
Porcine fibrin sealant
Microwave ablation of lung tumors
Complications
Radiation exposure

ABSTRACT

Purpose: This retrospective study aims to assess the efficacy of the combined application of electromagnetic navigation (EMN) and porcine fibrin sealant (PFS) in the microwave ablation (MWA) treatment of lung tumors.
Material and methods: In our department from January 2022 to August 2023, 73 patients underwent MWA under standard computed tomography (CT) guidance (CT group) or CT guidance with additional application of EMN and PFS (CT-EMN-PFS group), respectively. The basic data of patients were recorded and analyzed using the Student's *t*-test and Chi-square test between the two groups, and single factor and multi-factors binary logistic regression analyses were conducted to determine the risk factors of pneumothorax; meanwhile the incidence of complications, the number of CT scans and dose length product (DLP) were calculated and compared between the two guidance modes.
Results: Forty-seven patients underwent standard CT-guided MWA, meanwhile the remaining 26 patients underwent CT-guided MWA with combined application of EMN and PFS. The patients with lesions close to the bronchi or interlobar fissures, and underlying emphysema had a higher risk of pneumothorax, the corresponding odds ratio (OR) was 23.290 ($p = 0.004$), 33.300 ($p = 0.019$), and 8.007 ($p = 0.012$), respectively; the combined use of EMN and PFS could reduce the incidence of pneumothorax, with an OR of 0.094 (95 % confidence interval [CI]: 0.015–0.602, $p = 0.013$). The incidence rates of pneumothorax, pneumorrhagia and pleural effusion were 59.57 %, 61.70 %, and 19.15 % respectively in the CT group, and 30.77 %, 50.00 % and 7.69 % respectively in the CT-EMN-PFS group. The incidence rate of pneumothorax in the CT-EMN-PFS group was significantly lower than that in the CT group ($p = 0.017$). The median number of CT scans was 9 in the CT group and 5 in the CT-EMN-PFS group, respectively, meanwhile the median DLP was 1060.69 mGy*cm in the CT group and 600.04 mGy*cm in the CT-EMN-PFS group, respectively, which indicated there was a statistical difference in the amount of radiation exposure between the two groups ($p < 0.001$).

* Corresponding author. Medical School of Nantong University, Affiliated Hospital of Nantong University, Nantong, 226001, Jiangsu, China.
** Corresponding author. Nantong University. Deputy director of thoracic surgery, Affiliated Hospital of Nantong University, Nantong, 226001, Jiangsu, China.
*** Corresponding author. Anatomy teaching and research department, Nantong University. Nantong, 226019, Jiangsu, China.
E-mail addresses: chenjian.19881212@163.com (J. Chen), zhangxinhua@ntu.edu.cn (X. Zhang), tdfyzl@ntu.edu.cn (L. Zhong).
[1] These authors contributed equally to this work.

https://doi.org/10.1016/j.heliyon.2024.e37954
Received 12 April 2024; Received in revised form 13 September 2024; Accepted 13 September 2024
Available online 14 September 2024

Conclusion: The combined application of EMN and PFS demonstrates for the first time that there is a lower incidence rate of pneumothorax and significantly less radiation exposure during the MWA of the lung tumors.

1. Introduction

The local management of lung tumor patients who have long-term survival are becoming more active with the rapid development of immunotherapy and targeted therapy [1,2]. Surgical resection is considered a standard treatment for primary lung cancer or isolated pulmonary metastases in comparison with other local therapies such as radiotherapy, thermal ablation, cryoablation [3]. Nevertheless, two-thirds of primary lung cancer patients have received other minimally invasive alternative therapy owing to the existence of many contraindications to surgery [4]. In addition to surgery, the external beam radiotherapy is considered one of the standards for local treatment, but it has many radiation-related complications and can even lead to the development of radiation-related tumors in patients with long-term survival [5]. In local thermal ablation, a needle temperature of above 70 °c can achieve local haemostasis to a certain extent; however, in cryoablation, the risk of bleeding will be greater due to the use of extreme hypothermia to destroy cells [6].

Microwave ablation (MWA) is a common form of percutaneous thermal ablation, which has been increasingly used as a local treatment of lung tumors [7,8]. The mechanisms of cancer cell apoptosis induced by thermal ablation were discussed and examined in the rapidly developing areas [9,10]. Nevertheless, MWA can partially induce adverse events such as pneumothorax, pulmonary hemorrhage, bronchopleural fistula, and pleural effusion in the local treatment of lung tumors, this may be one of the reasons why MWA is not as widely used in the local treatment of lung cancers as radiofrequency ablation is widely used in the local treatment of liver cancers [11,12]. The risk factors associated with adverse events following percutaneous ablation of lung tumors have been identified. Additionally, the risk assessment of pneumothorax in lung tumors treated by percutaneous thermal ablation has been discussed [13,14]. However, pneumothorax after ablation of lung tumors is still mainly treated with closed thoracic drainage or hose suction in clinical practice [15]. At the same time, the percutaneous thermal ablation of lung tumor is typically performed under the guidance of computed tomography (CT) rather than magnetic resonance imaging (MRI) or ultrasound [16]. Therefore, radiation exposure is also a significant concern, particularly in cases where the tumor is inaccessible, which necessitates repeated CT scans, although radiation exposure dose can be reduced by changing the CT parameters such as tube voltage or current [17]. Therefore, developing a novel combined method to effectively reduce both the occurrence of complications such as pneumothorax and the CT radiation exposure is essential widespread promotion and application MWA of lung tumors in clinical practice.

Electromagnetic navigation (EMN) has been used for biopsy or ablation. Some studies reported that EMN has achieved some results in the precise positioning and the CT scan time reduction [18,19]. The main principle of EMN is based on reconstructing the first CT images to achieve the objectives of reducing the number of real-time CT scans required for needle adjustment during ablation or biopsy [20]. Although the application of EMN can assist inexperienced interventionalists in performing an effective ablation or biopsy to a certain extent [21], more studies are still needed to determine whether EMN can reduce the number of CT scans and radiation exposure in percutaneous ablation therapy [22]. The porcine fibrin sealant (PFS) adhesive, a common material that is used to reduce the deterioration of pneumothorax after thoracic surgical procedure [23,24], has been used as a comparably safe and effective method for biopsy in some reports [25,26]. In more cases, PFS is used for hemostasis [27,28]. PFS has also been used by some authors in the treatment of leaks or fistulae, such as cerebrospinal fluid leak [29] and alveolar pleural fistula [30], which have focused on soft tissue repair. However, there have been very few reports on the combined application of EMN and PFS in lung tumor ablation at present.

This study aimed to explore the scientific and clinical significance of combining EMN and PFS in the MWA of lung tumors through evaluating and comparing the safety and the radiation exposure of MWA treatment of lung tumors between simple CT guidance and CT guidance with additional application of EMN and PFS, thus contributing to the promotion of the application of modified MWA in the treatment of lung tumors in clinical practice.

2. Materials and methods

2.1. Patients

This study collected a total of 117 patients who had received MWA in the Department of Thoracic Surgery of Affiliated Hospital of Nantong University from January 2022 to August 2023. The treatment protocols of the patients were previously discussed by a comprehensive, multidisciplinary medical team. These patients were all informed of their conditions and treatment options before the operation, and they signed a written protocol additionally. Likewise, this retrospective study was approved by the ethics review committee of our hospital.

Inclusion criteria: (1) patients diagnosed with (primary or metastatic) lung tumor preoperatively or confirmed by postoperative pathology; (2) those with complete ablation assessed by intraoperative CT; (3) those with a postoperative follow-up time of not less than 6 months. Exclusion criteria: (1) patients without definite pathological examination results; (2) those who planned to undergo palliative treatment or whose operation was terminated early due to intolerance of complete ablation for reasons such as intraoperative pain; (3) those who were lost to follow up within six months for various reasons; (4) those who used EMN alone.

Finally, 47 (35 male, 12 female) patients underwent standard CT-guided MWA (CT group), meanwhile, 26 (17 male, 9 female) patients underwent CT-guided MWA with additional application of EMN and PFS (CT-EMN-PFS group). The CT-guided MWA combined with EMN and PFS was preferably used because the EMN technology has been applied in our department since the beginning of 2023. We applied EMN to reduce the number of repeated CT scans, thus decreasing the radiation dose. However, in the first month, the pneumothorax was present in 8 out of 10 patients, and two patients were treated with closed drainage; therefore, a common material PFS, which was often used in surgery to reduce pneumothorax, was additionally used. Fig. 1 shows the flow chart of patient enrolment. The majority of patients underwent standard CT-guided MWA in 2022, while the majority of patients underwent CT-guided MWA combined with EMN and PFS in 2023. The basic population information of the two groups is shown in Table 1.

2.2. *Equipment and reagents*

The devices used in both groups included CT (Discovery CT590 RT, GE HealthCare, America), a MWA therapeutic device (MTC-3C microwave ablation system, Vison-China Medical Devices R&D Center, China), Water-Cooled Microwave Ablation Probe (MTC-3CA-II13, Vison-China Medical Devices R&D Center, China), and biopsy needles (BioPince™ 18G*10 cm/18G*15 cm, Argon Medical Devices, America). Porcine Fibrin Sealant Kit (The product registration number was State Food and Drug Administration (Approval) No. S20100007, 5.0 ml, Guangzhou Bioseal Biotech Co.,Ltd., China) and Computed Electromagnetic Navigation (Thoracic & Abdominal Percutaneous Navigation System, AccuMed, China) were additionally applied in the CT-EMN-PFS group.

2.3. *Therapeutic process*

2.3.1. *Preparation before MWA*

The patients undergoing electrocardiogram (ECG), oxygen saturation, and non-invasive blood pressure monitoring were placed in a prone, lateral, or supine position on the CT table according to the location of the lung tumor. All patients should inhale low concentrations of oxygen and be given painkillers (dezocine 3–5 mg iv.) or sedatives (dexmedetomidine 0.5–1.0 μg/kg/h, iv-vp, lasting for 10 min) through a venous indwelling needle early if necessary.

2.3.2. *Normal CT-guided procedure*

According to the specific location of the tumor in the lung anatomical structure, we attached the grid paper on the corresponding body surface. Then the operator performed the first intraoperative whole lung CT scan, the parameters of which were as follows: (scan type: helical, 16 detector-row × 1.25 mm, pitch 1.375:1, slice thickness and slice interval 2.5 mm, tube voltage 120 Kv, tube current 50–400 mA under auto mA mode, noise coefficient 15.00, breathing mode: natural breathing, window width 1600 HU and window

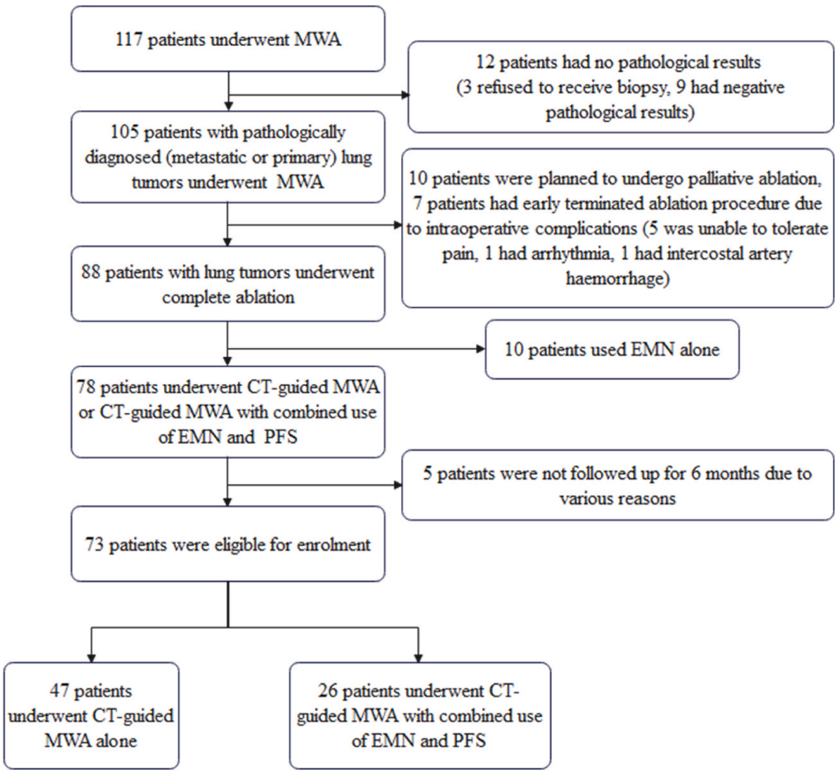

Fig. 1. Flow chart of patient screening. MWA, microwave ablation; EMN, electromagnetic navigation; PFS, porcine fibrin sealant; CT, computed tomography.

Table 1
Demographics of the patients, cancer characteristics and technical parameters.

Variables	All patients (n = 73)	CT group (n = 47)	CT-EMN-PFS group (n = 26)	*p* value
Age (years), mean ± SD	69.37 ± 9.85	68.65 ± 10.67	69.77 ± 9.47	0.647
Gender (n, %)				0.412
Male	52(71.23)	35(74.47)	17(65.38)	
Female	21(28.77)	12(25.53)	9(34.62)	
BMI (kg/m^2), mean ± SD	22.36 ± 3.18	22.31 ± 3.30	22.46 ± 3.02	0.852
Emphysema (n, %)				
+	38(52.05)	24(51.06)	14(53.85)	0.820
−	35(47.95)	23(48.94)	12(46.15)	
Radiographic characteristics (n, %)				0.099
Pure GGO	13(17.81)	6(12.77)	7(26.92)	
Mixed GGO	15(20.55)	9(19.15)	6(23.08)	
Solid	45(61.64)	32(68.08)	13(50.00)	
Tumor size(cm), mean ± SD				
Maximal diameter		2.41 ± 1.01	1.78 ± 0.80	0.008
Minimal diameter		1.86 ± 0.80	1.43 ± 0.73	0.027
Puncture path(cm), mean ± SD				
Skin-to-tumor length		7.15 ± 1.98	7.17 ± 1.70	0.972
Pleura-to-tumor length		2.94 ± 1.77	3.26 ± 1.70	0.451
Synchronous biopsy (n, %)				0.663
+	34(46.58)	21(44.68)	13(50.00)	
−	39(53.42)	26(55.32)	13(50.00)	
Previous history of lung surgery	11(15.07)	7(14.89)	4(15.38)	0.955
Close to bronchus	15(20.55)	9(19.15)	6(23.08)	0.691
Close to interlobar fissure	11(15.07)	7(14.89)	4(15.38)	0.955
Location (n, %)				
RUL	25(34.25)	14(29.79)	11(42.31)	
ML	2(2.74)	1(2.13)	1(3.85)	
RLL	14(19.18)	9(19.15)	5(19.23)	
LUL	23(31.50)	15(31.91)	8(30.77)	
LLL	9(12.33)	8(17.02)	1(3.85)	
Histology (%)				
Adenocarcinoma	44(60.27)	28(59.57)	16(61.54)	
Squamous carcinoma	13(17.81)	9(19.15)	4(15.38)	
Small-cell carcinoma	3(4.11)	2(4.26)	1(3.85)	
Metastases	13(17.81)	8(17.02)	5(19.23)	
Dose of MWA (W*min) mean ± SD		249.50 ± 75.54	184.02 ± 36.81	0.008

CT, computer tomography; EMN, electromagnetic navigation; PFS, porcine fibrin sealant; SD, standard deviation; BMI, body mass index; GGO, ground glass opacity; RUL, right upper lobe; ML, medial lobe; RLL, right lower lobe; LUL, left upper lobe; LLL, left lower lobe; MWA, microwave ablation.

level −650 HU). The physicians with more than five years of lung tumor ablation experience reviewed the CT images and selected percutaneous needle entry point (marked on the body surface) and treatment angle. After the skin around the marked point was disinfected by 1 % povidone-iodine and draped, 3–5 ml of 2 % lidocaine was used for local infiltration anesthesia from the skin to the partial pleura.

A step-by-step method was used to insert the biopsy needle to reach outside the parietal pleura, then a CT scan was performed, and the direction of needle insertion was adjusted in time according to the CT images. If the needle insertion path was correct, the needle was continuously inserted into the lung tissue; after CT scanning confirmed that the angle of needle insertion was correct, the needle could be continuously inserted until it reached the edge of the lesion, and then 2–3 tissues were harvested and sent for biopsy examination. Immediately after the biopsy needle was pulled out, the ablation antenna was inserted in an original direction according to the real-time CT images and gradually passed through the tumor. After the ablation antenna was put in place, its power cable was connected by the assistant, and the ablation dose (power value multiplied by time value) was then determined according to the tumor size and density.

The ablation procedure was completed when the ablation-induced ground glass halo had covered 5 mm around the tumor on CT images, this is defined as complete ablation. And the ablation antenna would be pulled out. Finally, CT images of the whole lung were acquired to assess the occurrence of postoperative complications, including pneumococcal, pulmonary hemorrhage, and pleura effusion. Thereafter, the patient would receive symptomatic treatment.

2.3.3. Electromagnetic navigation combined with porcine fibrin sealant procedure

Four magnetic poles connecting the cables were attached to the outside of the surgical range in the shape of a ladder, as shown in Fig. 2D. A magnetic field detector (Fig. 2F) was placed over the surgical area, covering the area encompassed by the four pole pieces, as shown in Fig. 2E. The magnetic navigation detector, pole pieces and EMN host computer were connected. The whole lung CT images (slice interval ≤ 2 mm) were collected and transmitted to the EMN host computer. Thereafter, the assistant adjusted the distance between the surface of the magnetic field detector and the pole pieces. When the EMN host computer received signals that met the

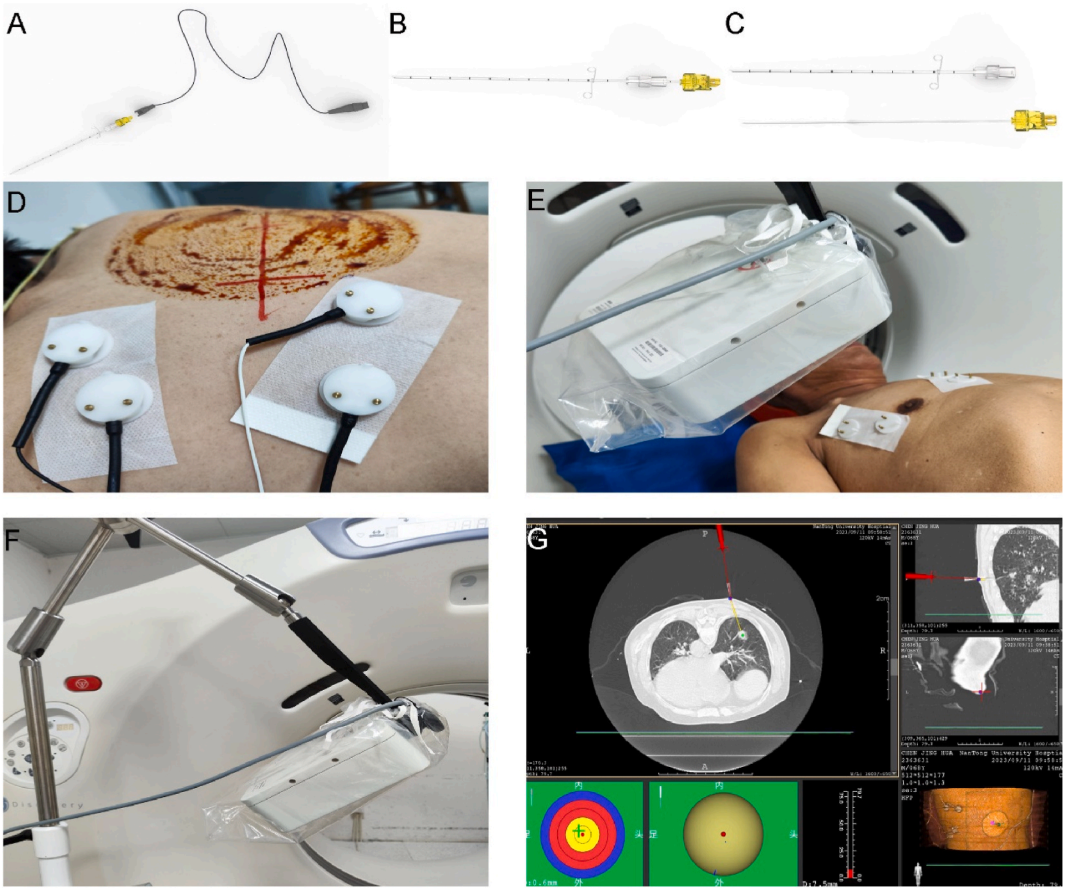

Fig. 2. Hardware and software of magnetic navigation system. A: a navigation needle was connected to the cable. B: a navigation needle was inserted into a trocar needle. C: The trocar needle and the navigation needle were placed separately. D: magnetic poles on the skin of a patient. E: Magnetic signal receiver directly facing the magnetic poles. F: Magnetic signal receiver. G: The real-time CT images in EMN software.

built-in criteria, three-dimensional (3d) reconstruction of CT images was performed subsequently. The needle entry point was selected under the guidance of the navigation needle after data modeling. After the skin around the selected point was disinfected and the local infiltration anesthesia was performed, the navigation needle, whose tip was made using magnetic navigation technology (Fig. 2A, B, C) inserted into a trocar needle, was punctured according to the computer-aided 3d reconstructed images until reaching a position at about 0.5–1 cm from the tumor edge. An intraoperative CT scan was performed to determine whether the direction of the entry needle conformed to the planned design. If the navigation needle was not well positioned, the position would be adjusted according to the planned design. When the planned design requirement was met, the navigation needle was removed and the ablation antenna was inserted into the trocar directly to pass through the tumor. Real-time intraoperative CT navigation images are shown in Fig. 2G. The synchronous biopsy was performed before the ablation if necessary.

The assistant used two syringes with a puncture cup to dissolve the freeze-dried powders of both PFS main adhesive and catalyst in their respective dissolution solutions (5 ml), and two soft needles were replaced respectively to add the main adhesive and catalyst into the left and right cavities of the dual cavity pipette respectively, and then a liquid dropper was installed for standby use. The apparatuses for preparing and injecting PFS are shown in Fig. 3A. The antenna was pulled out. and 1–2 ml of PFS was injected into the trocar after the ablation antenna was removed. The dual cavity pipette was pushed to deliver the PFS main adhesive and catalyst into the liquid dropper to synthesize PFS with adhesive effect on tissues, which was then injected into the cannula of the EMN needle trocar to enter into the lung tissue. Fig. 3B shows the actual assembled PFS injector filled with PFS main adhesive and catalyst. Fig. 4 shows the CT images of a 68-year-old male patient who underwent MAW with a combined application of EMN and PFS. The CT images were collected before, during and after the ablation (Fig. 4A–C). The areas indicated by the arrow in Fig. 4C and D and E were the line-shaped images of PFS on CT.

2.4. Outcome measures

The basic information of patients such as age, gender, body mass index (BMI), and previous history of lung surgery was collected. It was assessed whether the patient had emphysema based on the preoperative imaging data, and it was also determined whether the

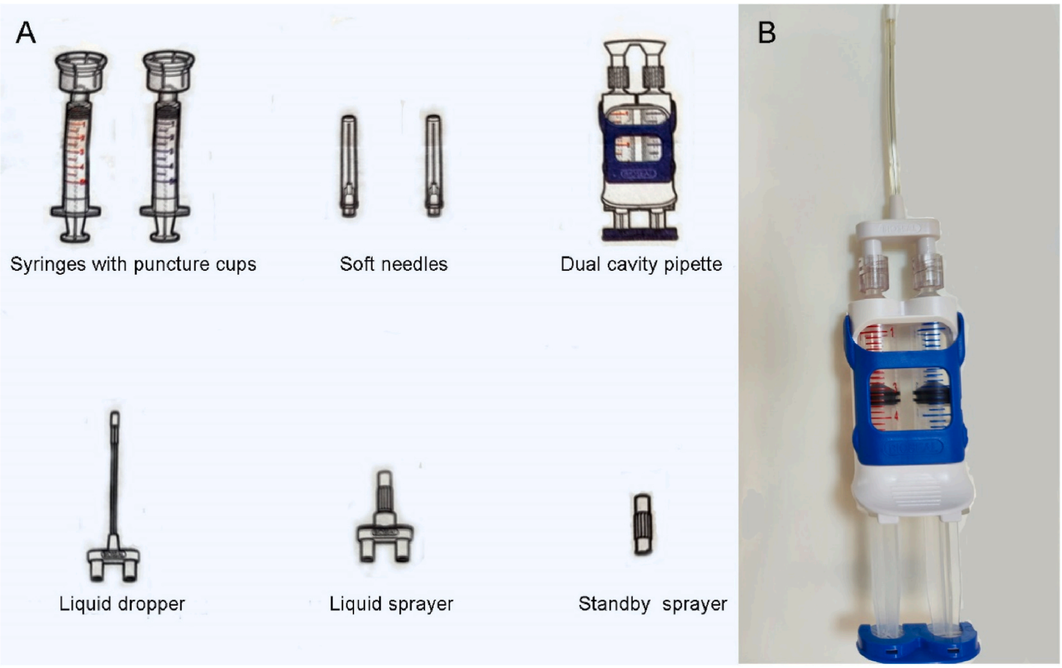

Fig. 3. Porcine Fibrin Sealant (PFS) Kit. A: The apparatuses for preparing and injecting PFS. B: Actual picture.

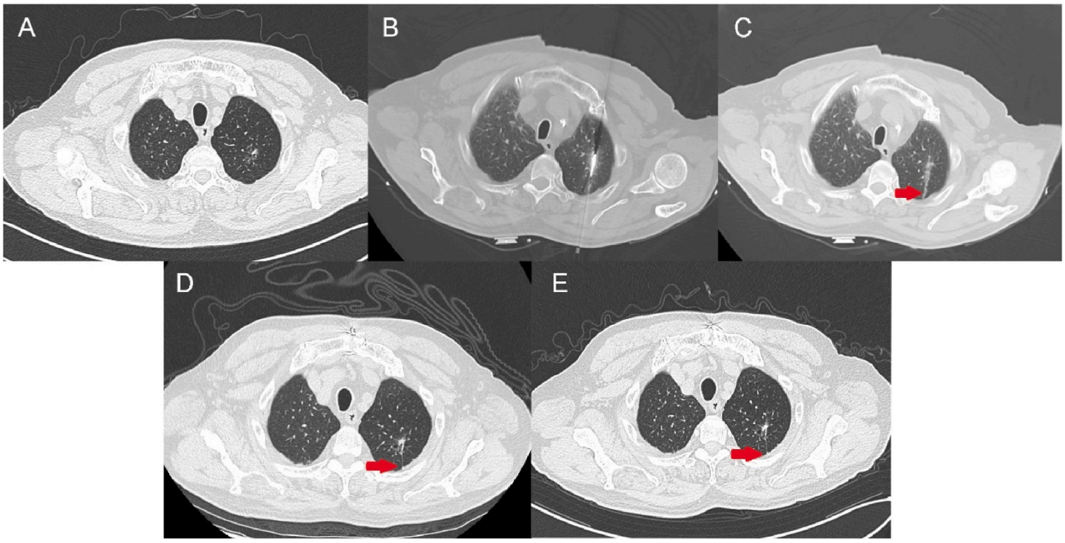

Fig. 4. Preoperative, intraoperative and postoperative CT images of a 68-year-old male patient undergoing CT-guided MAW with combined application of EMN and PFS. A: preoperative CT images; B: CT image taken after the microwave antenna was put in place during operation; C: real-time CT image right after operation; D: CT image taken at three months after operation; E: CT image taken at six months after operation. The area indicated by the arrow was the line-shaped image of PFS on CT.

lesion was close to a bronchus or interlobar fissure. The tumor size and location, radiographic characteristics, and length of the puncture path were collected from the intraoperative CT images. It was also determined whether the ablation procedure was synchronized with a biopsy (Table 1). The complications including pneumothorax, pneumorrhagia, pleural effusion, pain, and fever were recorded. The degree of pneumothorax was classified as that requiring chest tube placement and that requiring only oxygen inhalation and observation. Likewise, the amount of pneumorrhagia was determined according to the intraoperative images to decide using hemostatic drugs or observation treatment (Table 2). In addition, the radiation exposure and number of CT scans of the patients were collected and analyzed between the CT group and the CT-EMN-PFS group.

2.5. Statistical analysis

The continuous variables were expressed as mean ± standard deviation (SD). Otherwise, the non-normally distributed continuous data were reported as median (interquartile range [IQR]). The categorical variables such as gender, radiographic characteristics, complications, and tumor location were expressed as numbers and frequency. Chi-squared test was used to compare categorical variables, and the Student's *t*-test was used to compare the continuous variables. The incidence of complications, the number of CT scans, and radiation exposure were compared between two groups using the Mann-Whitney test. The possible risk factors for patients developing pneumothorax after ablation were also analyzed using single-factor logistic regression analysis, and then the screened factors with statistical significance ($p < 0.05$) were analyzed using multi-factors binary logistic regression analysis. The difference was considered statistically significant when a p-value was less than 0.05. SPSS version 20.0 and GraphPad Prism version 9.0 were applied for the statistical analyses.

3. Results

3.1. Basic characteristics of the patients and tumors

Overall, the mean age of the two groups (CT group and CT-EMN-PFS group) was 69.37 ± 9.85 years. There were more male patients (n = 52,71.23 %) in this study, and the BMI was 22.31 ± 3.30 kg/m^2 in the CT group and 22.46 ± 3.02 kg/m^2 in the CT-EMN-PFS group, respectively. There were no significant differences in age, sex, and BMI between the two groups, and p values were 0.647, 0.412, and 0.852, respectively.

The proportion of patients with emphysema was 51.06 % in the CT group and 53.85 % in the CT-EMN-PFS group, there was no statistically significant difference ($p = 0.820$). There was no statistically significant difference in the proportion of patients with previous lung surgery between the two groups ($p = 0.955$). Overall, 61.64 % of all lesions presented as solid nodules, and there was no statistical significance in imaging characteristics between the two groups ($p = 0.099$). However, the maximal and minimal diameters in the CT group were significantly greater than those in the CT-EMN-PFS group ($p = 0.008$, $p = 0.027$). The skin-to-tumor length and pleura-to-tumor length measured during the puncture process were 7.15 ± 1.98 cm and 2.94 ± 1.77 cm respectively in the CT group, 7.17 ± 1.70 cm and 3.26 ± 1.70 cm respectively in the CT-EMN-PFS group, there were no statistical differences between the two groups ($p = 0.972$, 0.451). The proportion of synchronous biopsy was 44.68 % in the CT group and 50.00 % in the CT-EMN-PFS group, respectively, with no statistical difference between the two groups ($p = 0.663$). The proportions of patients with lesions close to bronchus or interlobar fissures were 19.15 % and 23.08 % in the CT group and 14.89 % and 15.38 % in the CT-EMN-PFS group, respectively, with no statistically significant difference between the groups ($p = 0.691$,0.955). The common tumor locations in both groups were the right upper lung and left upper lung. The most common pathological type was adenocarcinoma.

3.2. Postoperative complications

Complications were graded using the Cirse classification system [31]. As shown in Table 2, the incidence rate of pneumothorax in the CT group (59.57 %) was significantly greater than that in the CT-EMN-PFS group (30.77 %). In terms of severity, 6 patients with pneumothorax required chest tube placement, and 22 patients with pneumothorax received oxygen inhalation and observation in the CT group; only 1 patient with pneumothorax had chest tube placement, and the remaining 7 patients with pneumothorax received oxygen inhalation and observation in the CT-EMN-PFS group, and there was a statistically significant difference between the two groups ($p = 0.017$). Only 2 patients had intrapulmonary hemorrhage and were treated with hemostatic drugs in the CT group, no intrapulmonary hemorrhage occurred in the CT-EMN-PFS group, and there was no statistically significant difference in the incidence rate of intrapulmonary hemorrhage between the two groups ($p = 0.122$); the incidence rate of pleural effusion occurring after ablation were 19.15 % in the CT group and 7.69 % in the CT-EMN-PFS group, respectively, and no statistically significant difference was detected between groups ($p = 0.19$). In addition, the combined application of EMN and PFS did not increase the risk of postoperative

Table 2
Complications of microwave ablations.

	CT group (n = 47)	CT-EMN-PFS group (n = 26)	*p* value
Pneumothorax (n, %)	28(59.57)	8(30.77)	0.017
CIRSE Grade 1–2	22(46.81)	7(26.92)	
CIRSE Grade 3(requiring chest tube)	6(12.76)	1(3.85)	
Pneumorrhagia (n, %)	29(61.70)	13(50.00)	0.122
CIRSE Grade 1–2	27(57.44)	13(50.00)	
CIRSE Grade 3 (Using hemostatic)	2(4.26)	0(0)	
Pleural Effusion (n, %)			0.190
CIRSE Grade 1–2	9(19.15)	2(7.69)	
Pain (n, %)			0.800
CIRSE Grade 1–2	16(34.04)	10(38.46)	
Fever (n, %)			0.760
CIRSE Grade 1–2	9(19.15)	4(15.38)	

CIRSE, Cardiovascular and Interventional Radiological Society of Europe.

fever or pain in tumor patients, as shown in Table 2.

3.3. *Risk factors for pneumothorax*

Single-factor logistic regression analysis was used to analyze the effects of factors such as age, BMI, gender, presence or absence of emphysema, tumor size (maximal and minimal diameters), length of the puncture path (skin-to-tumor length and pleura-to-tumor length), presence or absence of synchronous biopsy, previous history of lung surgery, proximity of lesions to bronchus or interlobular fissures, ablation dose, and combined application of EMN and PFS on the incidence of pneumothorax. Of which, the odds ratio (OR) of age, BMI, previous history of lung surgery, tumor size (minimal diameter), skin-to-tumor length, and pleura-to-tumor length were 1.008 (95 % confidence interval [CI]: 0.962–1.056), 1.024 (95%CI: 0.885–1.184), 1.280 (95%CI: 0.353–4.637), 1.843 (95%CI: 0.999–3.400), 1.006 (95%CI: 0.832–1.366), and 1.033 (95%CI: 0.792–1.347), respectively, and all p values were great than 0.05; therefore, these factors were excluded from subsequent analysis, the remaining factors with significant significance ($p < 0.05$) were further analyzed using multi-factors binary logistic regression analysis, the results showed that concurrent emphysema, the lesions close to the bronchus and interlobular fissure were high-risk factors for pneumothorax (all $p < 0.05$), and the combined application of EMN and PFS could significantly reduce the incidence of pneumothorax, with an OR of 0.094 (95%CI: 0.015–0.602, $p < 0.05$). See Table 3.

3.4. *Assessment of short-term local efficacy*

The patients were followed up and underwent enhanced CT examinations respectively at 3 and 6 months after the operation. No enhanced soft tissue shadow around the lesion on the enhanced CT image at 3 months after operation was defined as effective; no enhanced soft tissue shadow around the locally ablated lesion on the enhanced CT image at 6 months after operation and a decrease in the size or density of the lesion compared with before operation was defined as effective. Fig. 5 shows the CT images of a 60-year-old male patient with lung tumor with severe emphysema before, during and at 3 and 6 months after MWA respectively. In this case, the tumor was increased in size at 3 months (Fig. 5D) after MWA compared with the preoperative size (Fig. 5A–C), but there was no contrast enhancement of the tumor, and the follow up examination at 6 months (Fig. 5E) after MWA showed that the tumor began to shrink, which was defined as short-term effective. The 3 and 6-month local effective rates in the CT group were 93.62 % (effective in 44 cases) and 85.11 % (effective in 40 cases), respectively, and the 3 and 6-month effective rates in the CT-EMN-PFS group were 92.31 % (effective in 24 cases) and 84.62 % (effective in 22 cases), and there was no significant difference in short-term efficacy between the two groups ($p > 0.05$).

3.5. *Number of CT scans and radiation exposure*

Radiation exposure was expressed in terms of dose length product (DLP). DLP was used to evaluate the total radiation dose received by a subject after receiving a single CT exposure scan, and its calculation formula is as follows: $DLP = CTDIvol \times L$, where CTDIvol represents the volumetric dose index and L represents the Z-axis scan length, namely, the scan range. The minimal and maximum DLP were 280.68 mGy*cm and 2994.89 mGy*cm respectively in the CT group, and the minimum and maximum DLP were 218.33 mGy*cm and 1424.41 mGy*cm respectively in the CT-EMN-PFS group. The amount of radiation exposure was significantly reduced in the CT-EMN-PFS group, and there was an obvious statistical difference between the two groups ($p < 0.001$), as shown in Fig. 6A. Meanwhile, the maximum and minimum numbers of CT scans were 6 and 15 in the CT group, 4 and 7 in the CT-EMN-PFS group, respectively, as shown in Fig. 6B; the median number of CT scans was 9 in the CT group and 5 in the CT-EMN-PFS group, respectively; there was an obvious statistical difference between the two groups ($p < 0.001$).

4. Discussion

MWA is an important method for local treatment of lung tumor patients who cannot tolerate surgery [32,33], and such patients often have comorbidities such as emphysema, which also increase the risk of complications in MWA therapy, although most of the

Table 3
Risk factors for pneumothorax in the microwave ablations.

Factors	Univariate logistic regression		Multivariate logistic regression	
	OR (95%CI)	P	OR (95%CI)	P
Gender	3.409 (1.140–10.190)	0.028	1.791(0.333–9.625)	0.497
Tumor size (Maximal diameter)	1.710 (1.034–2.827)	0.037	0.266(0.035–2.034)	0.202
Emphysema	8.089 (2.840–23.043)	<0.001	8.007(1.580–40.577)	0.012
Synchronous biopsy	2.933(1.129–7.618)	0.027	3.290 (0.703–15.403	0.131
Bronchus*	5.667(1.442–22.274)	0.013	23.290(2.702–00.746)	0.004
Interlobar fissures*	13.846(1.668–114.964)	0.015	33.300(1.761–29.832)	0.019
Dose of MWA	1.586(1.100–2.286)	0.013	2.151(0.590–7.848)	0.246
PFS	0.302(0.109–0.833)	0.021	0.094(0.015–0.602)	0.013

OR, odds ratio; CI, confidence interval; Bronchus*, tumor close to bronchus; interlobar fissures*, tumor close to interlobar fissures.

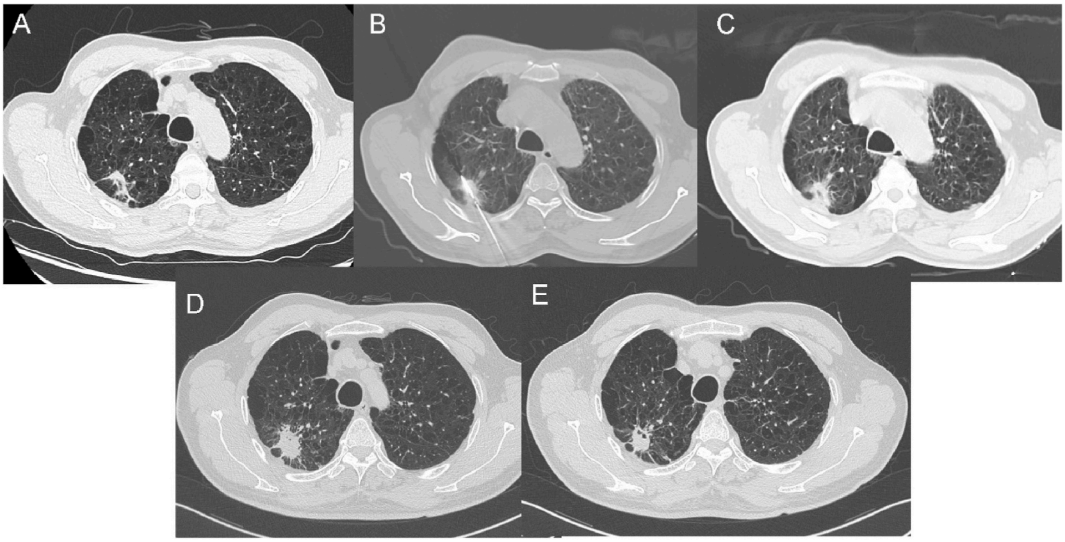

Fig. 5. Preoperative, intraoperative and postoperative CT images of a 60-year-old male patient with pulmonary emphysema undergoing CT-guided MAW with combined application of EMN and PFS. A: preoperative CT images; B: CT image taken after the microwave antenna was put in place during operation; C: real-time CT image right after operation; D: CT image taken at three months after operation; E: CT image taken at six months after operation.

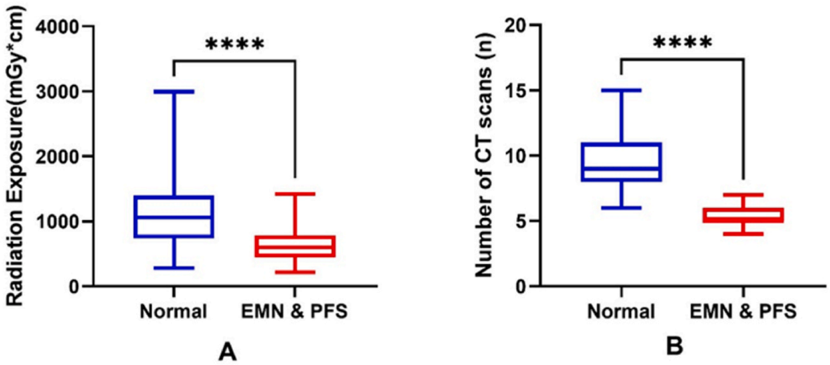

Fig. 6. Comparison of the amount of radiation exposure and the number of CT scans between the two groups. A: distribution of radiation exposure in the two groups; B: distribution of number of CT scans in the two groups.

complications are not fatal [34]. The life-threatening complications such as bronchopleural fistula, which had an incidence rate of less than 1 % in a previous study [35], did not occur in our study. We compared the incidences of complications such as pneumothorax, pneumorrhagia, pleural effusion, pain, and fever between the two groups, as shown in Table 2. Compared with previous reports on conventional CT-guided MWA [4,7,33], the combined application of EMN and PFS is relatively safe. Meanwhile, no significant difference in short-term efficacy between the two groups confirmed that the effect of the combined application on the local treatment would not be attenuated.

The rapid upgrading and application of computer technology in the medical field has made a lot of clinical examination and treatment technologies more accurate and mature, demonstrating a more and more simplified technology development trend [36]. Conventional CT guidance is often insufficient to meet the demand for different practical complex situations in clinical MWA. Previous report of the use of EMN did not suggest increasing the associated risk of complications such as pneumothorax [37]. Contrarily, in the other report about EMN-guided lung biopsy, the author considered that the occurrence of increased complication rate does not support the routine use of EMN [38]. The combined use of EMN and PFS in our study could reduce the incidence rate of pneumothorax, especially the incidence rate of severe pneumothorax requiring chest tube insertion, which may contribute to the use of PFS. This histological mechanism of pneumothorax after lung ablation in the porcine model has been described in the literature [39]. It has been found that the puncture path during imaging is a high-risk factor for pneumothorax after lung ablation [40]. The adhesive (PFS) is injected into the lung tissue through the cannula of the navigation needle, which can close the needle tract off and thus prevent pneumothorax formation. PFS is porcine blood derivative consisting of blood coagulation factors, fibrinogen, factor XIII (FXIII), thrombin, an antifibrinolytic agent and calcium chloride [29], and it mimics the final stages of the coagulation cascade to form a stable fibrin network, which acts as tissue adhesion. The similar mechanism was also found that an embolic agent can reduce the incidence of pneumothorax, thus leading to a lower chest tube insertion rate, and a correspondingly higher rate of sinus tract closure [41].

At first, we used EMN to solve the radiation exposure problem in MWA due to repeated CT image acquisition during CT-guided ablation, which is also a method to further optimize some advantages of thermal ablation in lung tumor treatment compared with the stereotactic ablative body radiotherapy (SABR) [42]. In the study by Q. Liu et al., the CT-guided percutaneous lung biopsy using an EMN system, which was also performed in our study, was compared with the conventional approach, the results indicated that this EMN system is a safe and effective technology, despite increasing the operation time [43]. The percutaneous or transbronchial protocol with EMN bronchoscopy guidance has been widely applied as a new technique for lung tumor biopsy and ablation [44,45]. G. Gadodia et al. proposed an augmented reality platform with a head-mounted display and electromagnetic tracking of instruments based on CT images, which was used for guiding percutaneous procedures [46]. All these studies are designed to guide the procedure in real-time and reduce the number of CT scans to some extent to facilitate the widespread application of lung tumor ablation or biopsy, whose findings are similar to those of our study. The ablation is performed under the guidance of the reconstructed CT images in the EMN system, which enables the real-time injection, and reduces the number of CT scans required for repeated needle adjustments especially when the lesion is small or deep, thus reducing the dose of radiation exposure. This is consistent with the principle of ensuring the safe use of medical radiation.

Meanwhile, multi-factors binary logistic regression analysis showed that the patients with concurrent emphysema and lesions close to the bronchus or interlobar fissures tended to have a higher incidence of pneumothorax, which is partially consistent with previous reports [34,35]. At the same time, we found that both the skin-to-tumor length and pleura-to-tumor length in the puncture path were low-risk factors for the incidence of pneumothorax. The reasons may be that: a shorter puncture path close to the visceral pleura would result in a higher incidence of pneumothorax, while a longer puncture path may lead to the fact that more normal lung tissues are damaged, and the damaged lung tissues may be closer to the bronchi, consequently resulting in a higher incidence of pneumothorax. Therefore, it may be unscientific to assume that a long puncture length will certainly reduce or increase the risk of pneumothorax. The size of the tumor does not affect the incidence of pneumothorax during the ablation therapy of metastatic pulmonary tumor [47]. Similarly, the final results of this study confirmed that the tumor size had no statistically significant effect on the incidence of pneumothorax after ablation therapy. Chi-squared test was used for comparison between the two groups, the incidence of pneumothorax was lower in the CT-EMN-PFS group ($p = 0.017$); similarly, the multi-factors binary logistic regression analysis indicated that the use of PFS could significantly reduce the incidence of pneumothorax, with an OR of 0.094 (95%CI: 0.015–0.602, $p = 0.013$). At present, few studies have explored the methods for preventing the major complications of ablation therapy, instead, some high-risk factors correlated to complications have been identified [48,49]. Therefore, the findings of this retrospective study have great significance in the prevention of pneumothorax after MWA of lung tumors.

Finally, multi-factors binary logistic regression analysis revealed that the synchronous biopsy was not a high-risk factor for pneumothorax. Therefore, if the patients are considered to have a possibility of malignant tumor on CT images and no clinical contraindications for MWA, the clinicians will prefer treating the patients with MWA and synchronous biopsy. As was mentioned in this report [50], synchronous biopsy is a safe and effective strategy that can reduce bleeding, radiation exposure dose, and the length of hospital stay.

This study has some shortcomings. The follow-up time is shorter, and it is unknown that whether the EMN and PFS affect the progression-free survival, thus a further study with a longer follow-up time is needed. No lethal complications occurred in this study, thus a further study with a larger sample size is needed to explore the effectiveness of this technique in reducing the occurrence of serious complications such as bronchopleural fistula. In addition, there is also a detection bias in tumor size; although the multi-factors binary logistic regression analysis indicated that the tumor size was not a high-risk factor for pneumothorax, the single-factor logistic regression analysis indicated that the tumor size was a high-risk factor for pneumothorax. Therefore, we will carry out a prospective randomized controlled study of this combined technique to address the bias in the future.

5. Conclusion

For MWA of lung tumors, the EMN technology can reduce the number of intraoperative CT scans and the dose of radiation exposure, and the PFS can decrease the incidence rate of pneumothorax, especially the chest tube placement rate. Thus, the combined application of navigation technology (EMN) and adhesive (PFS) is worth popularizing in clinical use. In particular, this study will provide reference value for promoting the application of MWA in medical clinics with limited experience, and guiding the inexperienced physicians to quickly master the application of MWA technology. Further studies for classifying patients with different risks of pneumothorax and different tumor locations are highly warranted in patients undergoing MWA treatment of lung tumors using EMN and PFS.

Ethics statement

This study was approved by The Ethics Committee of Affiliated Hospital of Nantong University, with the approval number:2023-L146. All participants have provided an informed consent for the publication of their data.

Data availability statement

The data cannot be disclosed online because the patients' privacy should be protected. However, partial of the data that support the discovery of this article can be obtained from the corresponding author via email.

Funding statement

No funding supports the works associated with this study.

CRediT authorship contribution statement

Jian Chen: Writing – review & editing, Writing – original draft, Data curation, Conceptualization. **Zaichun Shang:** Writing – original draft, Software, Methodology, Data curation. **Pengfei Jia:** Validation, Methodology. **Zhiming Chen:** Project administration. **Xiaowen Cao:** Data curation. **Xiao Han:** Methodology. **Xinhua Zhang:** Writing – review & editing, Conceptualization. **Lou Zhong:** Writing – review & editing, Project administration, Data curation, Conceptualization.

Declaration of competing interest

The authors declare that they have no known competing financial interests or personal relationships that could have appeared to influence the work reported in this paper.

Acknowledgments

The authors thank the patients and their families for participating in the study. They also thank Lou Zhong and Xinhua Zhang for their advice on study conception and other clinical staff in this research for their work without compensation.

References

[1] M. Miller, N. Hanna, Advances in systemic therapy for non-small cell lung cancer, BMJ 375 (2021) n2363, https://doi.org/10.1136/bmj.n2363.
[2] Q. Xu, F. Zhou, H. Liu, et al., Consolidative local ablative therapy improves the survival of patients with synchronous oligometastatic NSCLC harboring EGFR activating mutation treated with first-line EGFR-TKIs, J. Thorac. Oncol. 13 (9) (2018) 1383–1392, https://doi.org/10.1016/j.jtho.2018.05.019.
[3] L.F. Valle, R. Jagsi, S.N. Bobiak, et al., Variation in definitive therapy for localized non-small cell lung cancer among national comprehensive cancer network institutions, Int. J. Radiat. Oncol. 94 (2) (2015) 360–367, https://doi.org/10.1016/j.ijrobp.2015.10.030.
[4] R.F. Grasso, C. Bernetti, G. Pacella, et al., A comparative analysis of thermal ablation techniques in the treatment of primary and secondary lung tumors: a single-center experience, Radiol. Med. 127 (7) (2022) 714–724, https://doi.org/10.1007/s11547-022-01508-2.
[5] L.B. Travis, A.K. Ng, J.M. Allan, et al., Second malignant neoplasms and cardiovascular disease following radiotherapy, J. Natl. Cancer Inst. 104 (5) (2012) 357–370, https://doi.org/10.1093/jnci/djr533.
[6] M.M. Wrobel, P.P. Bourgouin, M. Abrishami Kashani, et al., Active versus passive thaw after percutaneous cryoablation of pulmonary tumors: effect on incidence, grade, and onset of hemoptysis, Am. J. Roentgenol. 217 (5) (2021) 1153–1163, https://doi.org/10.2214/AJR.21.25872.
[7] M.T. Tsakok, M.W. Little, G. Hynes, et al., Local control, safety, and survival following image-guided percutaneous microwave thermal ablation in primary lung malignancy, Clin. Radiol. 74 (1) (2019) e19–e26, https://doi.org/10.1016/j.crad.2018.09.014, 80.
[8] X. Ye, W. Fan, H. Wang, et al., Expert consensus workshop report: guidelines for thermal ablation of primary and metastatic lung tumors (2018 edition), J. Cancer Res. Ther. 14 (4) (2018) 730–744, https://doi.org/10.4103/jcrt.JCRT_221_18.
[9] L. Yu, H. Xie, H. Wang, et al., Microwave ablation induces abscopal effect via enhanced systemic antitumor immunity in colorectal cancer, Front. Oncol. 13 (2023) 1174713, https://doi.org/10.3389/fonc.2023.1174713.
[10] K.F. Chu, D.E. Dupuy, Thermal ablation of tumours: biological mechanisms and advances in therapy, Nat. Rev. Cancer 14 (3) (2014) 199–208, https://doi.org/10.1038/nrc3672.
[11] G. Olive, R. Yung, H. Marshall, et al., Alternative methods for local ablation-interventional pulmonology: a narrative review, Transl, Lung Cancer Res 10 (7) (2021) 3432–3445, https://doi.org/10.21037/tlcr-20-1185.
[12] P.J. Dempsey, C.A. Ridge, S.B. Solomon, Advances in interventional oncology: lung cancer, Cancer J. 22 (6) (2016) 393–400, https://doi.org/10.1097/PPO.0000000000000229.
[13] I. Tahir, A.M. Cahalane, J.A. Saenger, et al., Factors associated with hospital length of stay and adverse events following percutaneous ablation of lung tumors, J. Vasc. Interv. Radiol. 34 (5) (2023) 759–767.e2, https://doi.org/10.1016/j.jvir.2022.12.013.
[14] S.A. Kennedy, L. Milovanovic, D. Dao, et al., Risk factors for pneumothorax complicating radiofrequency ablation for lung malignancy: a systematic review and meta-analysis, J. Vasc. Interv. Radiol. 25 (11) (2014) 1671–1681.e1, https://doi.org/10.1016/j.jvir.2014.07.025.
[15] X. Ni, J.Q. Han, X. Ye, et al., Percutaneous CT-guided microwave ablation as maintenance after first-line treatment for patients with advanced NSCLC, Onco, Targets Ther 8 (2015) 3227–3235, https://doi.org/10.2147/OTT.S90528.
[16] A. Baisi, M. De Simone, F. Raveglia, et al., Thermal ablation in the treatment of lung cancer: present and future, Eur. J. Cardio. Thorac. Surg. 43 (4) (2013) 683–686, https://doi.org/10.1093/ejcts/ezs558.
[17] Y. Yamao, K. Yamakado, H. Takaki, et al., CT-fluoroscopy in chest interventional radiology: sliding scale of imaging parameters based on radiation exposure dose and factors increasing radiation exposure dose, Clin. Radiol. 68 (2) (2013) 162–166, https://doi.org/10.1016/j.crad.2012.05.020.
[18] R.S. Santos, A. Gupta, M.I. Ebright, et al., Electromagnetic navigation to aid radiofrequency ablation and biopsy of lung tumors, Ann. Thorac. Surg. 89 (1) (2010) 265–268, https://doi.org/10.1016/j.athoracsur.2009.06.006.
[19] L. Appelbaum, J. Sosna, Y. Nissenbaum, et al., Electromagnetic navigation system for CT-guided biopsy of small lesions, Am. J. Roentgenol. 196 (5) (2011) 1194–1200, https://doi.org/10.2214/AJR.10.5151.
[20] R.F. Grasso, F. Andresciani, C. Altomare, et al., Lung thermal ablation: comparison between an augmented reality computed tomography (CT) 3D navigation system (SIRIO) and standard CT-guided technique, Biology 10 (7) (2021) 646, https://doi.org/10.3390/biology10070646.
[21] Z. Chen, L. Meng, Y. Xiao, et al., Clinical application of optical and electromagnetic navigation system in CT-guided radiofrequency ablation of lung metastases, Int. J. Hyperthermia 41 (1) (2024) 230–333, https://doi.org/10.1080/02656736.2023.2300333.
[22] C.K. Narsule, R. Sales Dos Santos, A. Gupta, et al., The efficacy of electromagnetic navigation to assist with computed tomography-guided percutaneous thermal ablation of lung tumors, Innovations 7 (3) (2012) 187–190, https://doi.org/10.1097/IMI.0b013e318265b127.
[23] A. Gonfiotti, P.F. Santini, M. Jaus, et al., Safety and effectiveness of a new fibrin pleural air leak sealant: a multicenter, controlled, prospective, parallel-group, randomized clinical trial, Ann. Thorac. Surg. 92 (4) (2011) 1217–1224, https://doi.org/10.1016/j.athoracsur.2011.05.104, discussion 1224-1225.
[24] T.B. Pedersen, J.L. Honge, H.K. Pilegaard, et al., Comparative study of lung sealants in a porcine ex vivo model, Ann. Thorac. Surg. 94 (1) (2012) 234–240, https://doi.org/10.1016/j.athoracsur.2012.03.050.

[25] T. Petsas, D. Siamblis, C. Giannakenas, et al., Fibrin glue for sealing the needle track in fine-needle percutaneous lung biopsy using a coaxial system: Part II–Clinical study, Cardiovasc. Intervent. Radiol. 18 (6) (1995) 378–382, https://doi.org/10.1007/BF00338305.
[26] R.A. Chisholm, S.N. Jones, W.R. Lees, Fibrin sealant as a plug for the post liver biopsy needle track, Clin. Radiol. 40 (6) (1989) 627–628, https://doi.org/10.1016/s0009-9260(89)80326-5.
[27] F. Izzo, R. Palaia, V. Albino, et al., Hepatocellular carcinoma and liver metastases: clinical data on a new dual-lumen catheter kit for surgical sealant infusion to prevent perihepatic bleeding and dissemination of cancer cells following biopsy and loco-regional treatments, Infect. Agent. Cancer 10 (2015) 11, https://doi.org/10.1186/s13027-015-0006-0.
[28] L. Segger, M.H. Lerchbaumer, F. Collettini, et al., Percutaneous computed tomography (CT) fluoroscopy-guided biopsy of the spleen using fibrin glue as a sealant, Diagnostics 14 (2) (2024) 162, https://doi.org/10.3390/diagnostics14020162.
[29] S. Du, J. Zhao, G. Qiao, et al., Cost-effectiveness analysis of the application of a porcine-derived fibrin sealant for the treatment of cerebrospinal fluid leak in China, Clin. Ther. 44 (4) (2022) 575–584, https://doi.org/10.1016/j.clinthera.2022.02.010.
[30] A. Fiorelli, I. Odierna, D. Scarano, et al., Combined intrapleural and intrabronchial injection of fibrin glue for closing alveolar pleural fistula: a case report, J. Cardiothorac. Surg. 14 (1) (2019) 171, https://doi.org/10.1186/s13019-019-0987-7.
[31] M. Venturini, M. Cariati, P. Marra, et al., CIRSE standards of practice on thermal ablation of primary and secondary lung tumours, Cardiovasc. Inter. Rad. 43 (5) (2020) 667–683, https://doi.org/10.1007/s00270-020-02432-6.
[32] R. Iezzi, R. Cioni, D. Basile, et al., Standardizing percutaneous Microwave Ablation in the treatment of Lung Tumors: a prospective multicenter trial (MALT study), Eur. Radiol. 31 (4) (2021) 2173–2182, https://doi.org/10.1007/s00330-020-07299-2.
[33] Y. Ni, G. Huang, X. Yang, et al., Microwave ablation treatment for medically inoperable stage I non-small cell lung cancers: long-term results, Eur. Radiol. 32 (8) (2022) 5616–5622, https://doi.org/10.1007/s00330-022-08615-8.
[34] H. Fan, X. Xie, Z. Pang, et al., Risk assessment of pneumothorax in colorectal lung metastases treated by percutaneous thermal ablation: a multicenter retrospective cohort study, Int. J. Surg. 110 (1) (2024) 261–269, https://doi.org/10.1097/JS9.0000000000000782.
[35] M.S. Kim, H.P. Hong, S.Y. Ham, et al., Complications after 100 sessions of cone-beam computed tomography-guided lung radiofrequency ablation: a single-center, retrospective experience, Int. J. Hyperthermia 37 (1) (2020) 763–771, https://doi.org/10.1080/02656736.2020.1784472.
[36] F. Banovac, P. Cheng, E. Campos-Nanez, et al., Radiofrequency ablation of lung tumors in swine assisted by a navigation device with preprocedural volumetric planning, J. Vasc. Interv. Radiol. 21 (1) (2010) 122–129, https://doi.org/10.1016/j.jvir.2009.09.012.
[37] M. Lanouzière, O. Varbédian, O. Chevallier, et al., Computed tomography-navigation™ electromagnetic system compared to conventional computed tomography guidance for percutaneous lung biopsy: a single-center experience, Diagnostics 11 (9) (2021) 1532, https://doi.org/10.3390/diagnostics11091532.
[38] J. Thiboutot, N.J. Pastis, J. Akulian, et al., A multicenter, single-arm, prospective trial assessing the diagnostic yield of electromagnetic bronchoscopic and transthoracic navigation for peripheral pulmonary nodules, Am. J. Respir. Crit. Care Med. 208 (8) (2023) 837–845, https://doi.org/10.1164/rccm.202301-0099OC.
[39] J. Izaaryene, F. Cohen, P. Souteyrand, et al., Pathological effects of lung radiofrequency ablation that contribute to pneumothorax, using a porcine model, Int. J. Hyperthermia 33 (7) (2017) 713–716, https://doi.org/10.1080/02656736.2017.1309577.
[40] M. Lignieres, N. Roux, R. Giorgi, et al., Persistent pathways after lung radiofrequency ablation as a risk factor of drain placement, Int. J. Hyperthermia 33 (6) (2017) 659–663, https://doi.org/10.1080/02656736.2017.1288931.
[41] T. de Baère, Pneumothorax and lung thermal ablation: is it a complication? Is it only about tract sealing? Cardiovasc. Intervent. Radiol. 44 (6) (2021) 911–912, https://doi.org/10.1007/s00270-021-02817-1.
[42] R.A. Watson, I. Tol, S. Gunawardana, et al., Is microwave ablation an alternative to stereotactic ablative body radiotherapy in patients with inoperable early-stage primary lung cancer? Interact, Cardiovasc. Thorac. Surg. 29 (4) (2019) 539–543, https://doi.org/10.1093/icvts/ivz123.
[43] Q. Liu, X. Guo, Z. Wang, et al., Computed tomography-guided percutaneous lung biopsy with electromagnetic navigation compared with conventional approaches: an open-label, randomized controlled trial, J. Thorac. Imag, Published online November 20, https://doi.org/10.1097/RTI.0000000000000763, 2023.
[44] Y. Li, W. Chen, F. Xie, et al., Novel electromagnetic navigation bronchoscopy system for the diagnosis of peripheral pulmonary nodules: a prospective, multicentre study, Thorax 78 (12) (2023) 1197–1205, https://doi.org/10.1136/thorax-2022-219664.
[45] W.Y. Chan Joyce, W.H. Lau Rainbow, C.L. Ngai Jenny, et al., Transbronchial microwave ablation of lung nodules with electromagnetic navigation bronchoscopy guidance—a novel technique and initial experience with 30 cases, Transl, Lung Cancer R 10 (4) (2021) 1608–1622, https://doi.org/10.21037/tlcr-20-1231.
[46] G. Gadodia, J. Yanof, A. Hanlon, et al., Early clinical feasibility evaluation of an augmented reality platform for guidance and navigation during percutaneous tumor ablation, J. Vasc. Interv. Radiol. 33 (3) (2022) 333–338, https://doi.org/10.1016/j.jvir.2021.11.014.
[47] L. Zhu, J. Huang, C. Jin, et al., Retrospective cohort study on the correlation analysis among peri-procedural factors, complications, and local tumor progression of lung tumors treated with CT-guided microwave ablation, J. Thorac. Dis. 15 (12) (2023) 6915–6927, https://doi.org/10.21037/jtd-23-1799.
[48] A.M. Splatt, K. Steinke, Major complications of high-energy microwave ablation for percutaneous CT-guided treatment of lung malignancies: single-centre experience after 4 years, J. Med. Imaging Radiat. Oncol. 59 (5) (2015) 609–616, https://doi.org/10.1111/1754-9485.12345.
[49] Y. Lamfichekh, V. Lafay, J. Hamam, et al., Score to predict the occurrence of pneumothorax after computed tomography-guided percutaneous transthoracic lung biopsy, J. Thorac. Imaging 38 (5) (2023) 315–324, https://doi.org/10.1097/RTI.0000000000000729.
[50] J. Zhang, K. Xu, K. Du, et al., Simultaneous percutaneous microwave ablation and biopsy for highly suspected malignant pulmonary nodules: a retrospective cohort study, Quant. Imaging Med. Surg. 13 (10) (2023) 7214–7224, https://doi.org/10.21037/qims-23-138.